Fuel 332 (2023) 125674

Contents lists available at ScienceDirect

Fuel

journal homepage: www.elsevier.com/locate/fuel

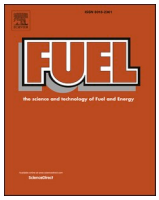

Full Length Article

Characterization of water droplets size distribution in aviation turbine fuel: Ultrasonic homogeniser vs high shear speed mixer

Judith Ugbeh-Johnson [a,*], Mark Carpenter [a], Nonso Evaristus Okeke [b], Nathalie Mai [a]

[a] Centre for Defence Chemistry, Cranfield University, Shrivenham SN6 8LA, United Kingdom
[b] School of Water, Energy, and Environment, Cranfield University, Cranfield, MK43 0AL, United Kingdom

ARTICLE INFO

Keywords:
Droplets size
Stokes law
Aviation fuels
Fuel systems
Shedding
Jet fuel
Aircraft
Emulsion

ABSTRACT

Pumps, pressure drops across fittings, and flight operations (such as turning manoeuvres, take-off, and landing) are some of the many sources of turbulence mixing and shearing in aircraft fuel systems, therefore, making it an inevitable condition. Literature established that shearing conditions would influence the droplets and droplets size distribution in an oil/water emulsion. So, low intensity shearing conditions could be beneficial as it promotes droplets coalescence, which could be a driving force for a weak emulsion. However, to date no experimental data has shown the influence homogenising intensity and total water content has on dispersed water droplets size distribution in aviation fuel. Therefore, to expand knowledge of quantification of measurements of dispersed water droplets in aviation fuel, this study characterizes dispersed water droplets in aviation turbine fuel, varying available laboratory homogenising devices and water content. Results presented show that droplets count increases with water concentration and shearing effect. To provide more statistical evidence, kurtosis and skew values were calculated from the extrapolated data and compared with data from a hexanol/water mixture given that hexanol is likely to form a stable emulsion. Experimental results show that the higher the homogenising intensity the more stable the emulsion is likely to be with a higher kurtosis and skew value close to that for the hexanol/water mixture. Therefore, observations show that mild shearing conditions (high shear mixing in this case) could help promote droplets coalescence, leading to a better separation ability.

1. 1. Background of study

Condensation, refuelling operations and maintenance operations are means in which water can get into jet fuel. The problem of water in fuel has been a major cause for concern in the aviation industry as it can lead to safety issues. Water in fuel can disperse as droplets that can eventually freeze at low temperatures, potentially leading to fuel flow restriction [1]. Water can enter the fuel by different mediums like during refuelling operations, maintenance and other flight operations. Take-off, landing, turning manoeuvres are some of the many flight operations that contribute to mixing and shearing the fuel in aircraft fuel systems, therefore, making it an inevitable condition. Work by Noor et al. suggested that mild shearing could be beneficial as it promotes droplets coalescence, which could be a driving force for a weak emulsion [2]. Additionally, findings by [3] and [4] established that shearing conditions would have a tremendous effect on the droplets size variation in an oil/water emulsion; the higher the shearing effect (energy input), the greater the fuel/water dispersion and the probability of smaller droplets size production [3–5]. It has been established in the literature that ice accretion is dependent on the amount of water in fuel, temperature and size of supercooled water droplets of the fuel [6–10]. Goodarzi et al. suggested that droplets interact with each other and deform from the original spherical shape at high water concentrations of dispersed phase; the researchers suggested correction factors as a function of the dispersed phase volume fraction to consider the deformation of droplets. The results obtained from work by Goodarzi et al. show that there is a good separation in the water in oil mixture with higher total water content [3]. As a result, the influence of water content on the average

Abbreviations: C, Volume concentration; CF, Cumulative frequency; d, Mean droplets size diameter (μm); DSD, Droplets size distribution; g, Acceleration due to gravity (m/s^2); HSM, High shear mixer; KF, Karl Fischer; n, Number ranging from 2.4 to 4.65 for increasing particle Reynolds Number; ppm, Parts per million; rpm, Revolutions per minute; UPs, Ultrasonic processor; V, Terminal velocity (m/s); ViPA, Visual Process Analyser; WVA, Weighted volume average (μm); s, Density of fuel (kg/m^3); SASOL, South African Synthetic Oil; s.d, Standard deviation; U, Settling velocity (m/s).

* Corresponding author.
E-mail address: j.ugbeh@cranfield.ac.uk (J. Ugbeh-Johnson).

https://doi.org/10.1016/j.fuel.2022.125674
Received 12 January 2022; Received in revised form 9 August 2022; Accepted 15 August 2022

droplets size distribution is evaluated to demonstrate the impact of water content and time on the water droplets size and count distribution.

Water in aviation fuel has been a long-standing area of concern in the aviation industry [11–17]. There are three different forms in which water could exist in aviation fuel; as dissolved water, dispersed water and free water [8,9]. Water that has dissolved in aviation fuel, exists as molecules that could precipitate out of the solution as suspended or free droplets at cold temperatures. Suspended water droplets can be formed when the water solubility limit of the aviation fuel has been exceeded or be formed by mechanical agitation by a jet pump, during aircraft manoeuvres or pressure refuelling [18,19]. Suspended water droplets take time to settle out or coalesce but eventually form free water that settles at the bottom of the tank [10,20,21]. Droplets of a few microns can also be a problem and previous work done in this area has shown that free water has a droplets size range of 20 – 30 μm, whilst suspended water droplets have a droplets size range of up to 13 μm [22,23].

Detailed visual droplets counting procedures have been reported in ASTM D7619-17 and ASTM D8166-21a to assist in addressing safety issues and also improve categorisation and quantification of water contamination in fuel [23,24]. Yet, the mechanism of water droplets formation and uptake in aviation fuel is an area that lacks detail in the literature. It is paramount to understand the fundamental properties that could influence the process and behaviour of water in aviation fuel. Previous study of water-in-oil emulsion has demonstrated that the DSD is one such factor that could play a key role in characterising water behaviour in an emulsion [3]. Also, a recent study conducted by Ugbeh et al investigated the droplets size distribution in five sustainable aviation fuels (SASOL-Synthetic paraffinic kerosine, Syntroleum gas to liquid, Hydroprocessed esters and fatty acids, Alcohol-to-jet fuel, and farnesane) and compared the results with the distribution of convention jet fuel using a high shear mixer. Observations showed that water droplets size is influenced by the chemical composition of the fuel and droplets sizes in the range of 3 – 6 μm were noticed for the different fuel types explored [25]. Therefore, this present study is aimed at characterizing the droplets size and frequency distribution by laying emphasis on the following objectives: (a) To demonstrate, based on theoretical assumptions, that droplets size/frequency in jet fuel distribution is governed by shearing conditions. (b) To demonstrate the impact of water content and time on the water droplets size and count distribution. A notable point is that the choice of added water content was arbitrary for this study; the importance was having a considerable and comparable amount of free water as free water content can be affected by the total water content of the fuel.

2. Experimental procedure

Particle Image analyser, the Jorin Visual Process Analyser (ViPA): The ViPA was manufactured by Jorin ltd., Whetstone, Leicester, England. The imaging analysis is a continuous cycle employing a recording microscope that displays real-time images of particles in the fluid and categorizes particle of interest. The particle size detection limit is a minimum of ~ 1.5 μm and a maximum of ~ 300 μm. Experimental information was collected for approximately 3900 s and recorded as counts per 39 s. The ViPA unit allows the user to define parameters that enable it to differentiate particles based on size or shape. The unit can quantify data on a number of parameters allowing the user to decide which parameters fit the purpose of the work. In this study, the size, and volume parameters were analysed.

The mean droplets size was calculated using the equation below.

$$\underline{D}_{[1,0]} = \frac{\sum_{i=0}^{\infty} n_i d_i}{\sum_{i=0}^{\infty} n_i} \tag{1}$$

Also, the ''De Brouckere mean diameter also referred to as weighted volume average (WVA)'' was employed for as it takes into account the mass and volume of a given distribution [26,27]. The equation for the weighted- volume average $\underline{D}_{4,3}$ can be written as:

$$\underline{D}_{[4,3]} = \frac{\sum_{i=0}^{\infty} n_i d_i^4}{\sum_{i=0}^{\infty} n_i d_i^3} \tag{2}$$

To improve confidence in the experimental data generated from the DSD, further statistical analysis was conducted by computing the kurtosis and skewness [2825]. Kurtosis statistically measures the sharpness of the tail on the distribution curve and the combined weight of the data points relative to the mid-section of the distribution curve. Meanwhile, the skew value measures the distortion or asymmetry of the DSD. If a data set has perfect symmetry, then the skew value is expected to be near zero. The skew parameter can have either a negative or a positive value. A distribution is said to be negatively skewed when the majority of its data points is skewed to the left or, in the case of this work, where there exist outliers or peaks at larger diameter in the distribution (coalescence = collison of small droplets to form larger ones). The equations for skewness and kurtosis are:

$$Skewness\ (sk) = \frac{n}{(n-1)(n-2)} \sum_{i=1}^{n} \left(\frac{di - n}{s.d}\right)^3 \tag{3}$$

$$Kurtosis\ (k) = \frac{n(n+1)}{(n-1)(n-2)(n-3)} \sum_{i=1}^{n} \left(\frac{di - n}{s.d}\right)^4 - 3\frac{(n-1)^2}{(n-2)(n-3)} \tag{4}$$

s.d = standard deviation, d = mean droplets size diameter.

Procedure adopted for producing dispersed water in aviation fuel: The fuel-water sample was prepared using a 100 mL measuring cylinder ~ 32 mm diameter to accommodate the homogeniser and the stirrer. A clean and dry 100 mL measuring cylinder was filled with 100 mL of fuel .0.1 mL or 0.05 mL of water was added to the 100 mL fuel, depending on the experiment. Blending was done using either a high shear mixer (HSM) or an ultrasonic horn as seen in Fig. 1 below.

The fuel was subjected to different shearing methods for the purpose of comparison to analyse the shearing effect on the water droplets size distribution and counts. The ultrasonic horn (UP200S model) has a frequency of 24 kHz, nominal power output of 200 W, and amplitude adjustable from 20 to 100 %. Tests were conducted using conventional Jet A-1 which is a hydrocarbon mixture consisting mainly of straight and branched chain paraffins (C8 to C16), naphthenes and aromatics. Table 1 summarises sets of test condition conducted for this study.

The ultrasonic processor (UP200S model) converts an electrical signal into a high frequency vibration, producing high-intensity ultrasonic waves which form small bubbles or voids in the liquid that collapse quickly thereby disrupting the liquid molecules and enhancing mixing of the water and fuel. For the X 620 HSM, shearing effect can be changed by altering the impeller speed. For the present study, the shearing rate was set to a constant speed of 11,000 rpm and allowed to homogenise for 60 s.

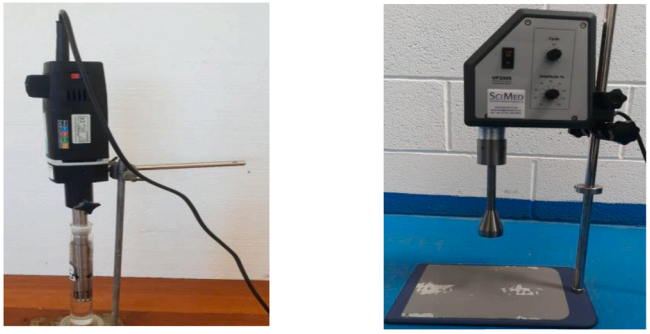

a) b)

Fig. 1. Instruments used for water dispersion a) X 620 high shear mixer: b) UP200S Ultrasonic processor.

Table 1
Test conditions using conventional Jet A-1 fuel.

S/N	Experiment	Weight % Water added	Shearing effect
1	Phase 1 experiments	0.05	Ultrasonic horn
2		0.05	High shear mixer
3		0.1	Ultrasonic horn
4		0.1	High shear mixer
5	Phase 2 experiments	0.02	High shear mixer
6		0.05	High shear mixer
7		0.1	High shear mixer
8		1	High shear mixer

As soon as the emulsion has been prepared, the ViPA system was set in place to begin analysis. Fig. 2 shows the schematic of the set up.

The experimental method for the HSM only was incorporated to this work from previous study conducted by Ugbeh et al [25]. As seen in Fig. 2, the blue flexible "inlet'' tube was positioned at the centre of the cylinder while the orange flexible passage "outlet' tube was positioned at the bottom of the cylinder. The peristaltic pump was switched on and the experimental analysis began when the ViPA system started. The main source of error is from the measurement of the water droplets size distribution using the Jorin ViPA with an accuracy of ± 2 % full scale and repeatability ± 1.5 %. Snapshots were taken at the start and finish of the experiment for comparison. A Karl Fischer coulometer was employed for the water content analysis. Analysis was done immediately after the emulsion has been prepared. Experiments was conducted in separate phases. Phase 1 examined the effects of mechanical agitation and phase 2 examined the effects of total water content. For the phase 2 experiments, a known amount of distilled water (0.02 %, 0.05 %, 0.1 %, and 1 %) was added to the fuel and homogenized for 60 s at 11,000 rpm using an X 620 high shear mixer.

3. Results and discussion

Effects of shearing conditions: Flight operations such as turning manoeuvres, take-off and landing are some of the many sources of turbulence mixing and shearing in aircraft fuel systems, therefore, making it an inevitable condition. Work by Noor et al. suggested that mild shearing conditions could be beneficial as it promotes droplets coalescence, which could be a driving force for a weak emulsion [2]. Additionally, Findings by [3] and [4] established that shearing conditions would have a tremendous effect on the droplets size variation in oil/water emulsion. Water droplets merge to form larger droplets during coalescence. It is an irreversible process that reduces the number of water droplets and ultimately results in demulsification. High flocculation rates, high water concentration, interfacial tension, and interfacial viscosities promote coalescence [25]. There are several factors that drive droplets coalescence. These can be summarised as the number of droplets/droplets collisions, relative velocity at which droplets collisions take place, relative size of the droplets which are colliding, electrical charges surrounding the water droplets (their zeta potential), oil/water interfacial tension, thickness and stability of the film on the surface of the water droplets, and viscoelastic properties of the stabilising film on the surface of the water droplets. Consensus has it that the higher the shearing effect (energy input), the greater the fuel/water dispersion and the probability of smaller water droplets size production [3–5]. To investigate if droplets size/frequency distribution in jet fuel is governed by shear conditions, water droplets produced by a high shear mixer were compared to those produced by ultrasonic dispersion for this study. The result from this set of experiments is given in Figs. 1 and 2.

Fig. 3 shows a images captured by the ViPA at the start of the Phase 1 experiment. As seen from Fig. 3, smaller droplets were formed with the ultrasonic processor compared to the HSM. Fig. 4 shows the droplets frequency distribution for the ultrasonic and HSM cases explored.

The skew to the right in the droplets distribution in Fig. 4 a and b shows that both shearing conditions exhibit a positive skewness as the right-hand tail is longer than the left. The droplets size distribution for mixtures with higher shear conditions (ultrasonic horn) is characterised by their near monomodal (single peak) distribution and a slightly higher kurtosis value of 13.45. Droplets size distribution for a mixture prepared with a milder shear rate, HSM, is characterised by their almost evident second peak and a lower kurtosis value of 7.5. Also, as anticipated, the skewness value is lower for the high shear mixer distribution (2.86) compared to the ultrasonic horn distribution (3.57).

On mixing with the ultrasonic horn, a high intensity shearing effect is generated as it introduces a lot of energy into the system, thereby producing smaller droplets and a single mode distribution as seen in Fig. 4c and d; bigger droplets were formed when the high shear mixer was employed. For clarity, Fig. 4a and b demonstrate the droplets size distribution with smoothed kernels. On shearing with the HSM, a collision of small drops with a diameter around 2 μm gives rise to larger droplets around 5 μm. Therefore, the distribution is observed in Fig. 4 a; with one large peak denoted as centred around 3 μm and small broadband around 6 μm. However, for the emulsion formed using the ultrasonic horn, which in theory introduces more energy into the system (higher shear rate), a monomodal distribution was observed as seen in Fig. 4b, with one narrow peak around 3 μm. Also, between both cases, the maximum value of volume-weighted mean and mean diameter is reached in the HSM case (green and blue vertical bar, respectively) because of the presence of larger droplets sizes and counts (as seen in Fig. 4). Therefore, it can be concluded that increased shear conditions lead to a decrease in the mean size droplets (4 to 2.9 in this case) and leads to a narrower droplets size distribution as seen in Fig. 4c and d.

The plots in Fig. 5a, and b show that a lesser droplets count was

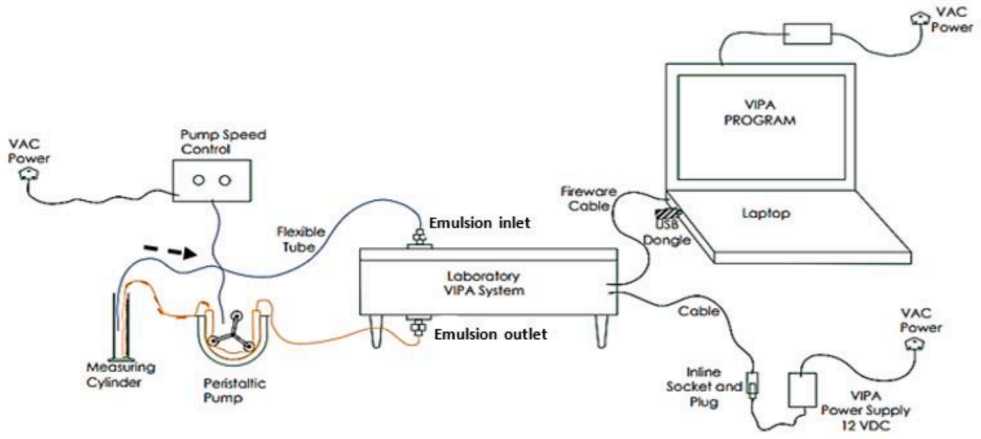

Fig. 2. ViPA analysis unit experimental set up [25].

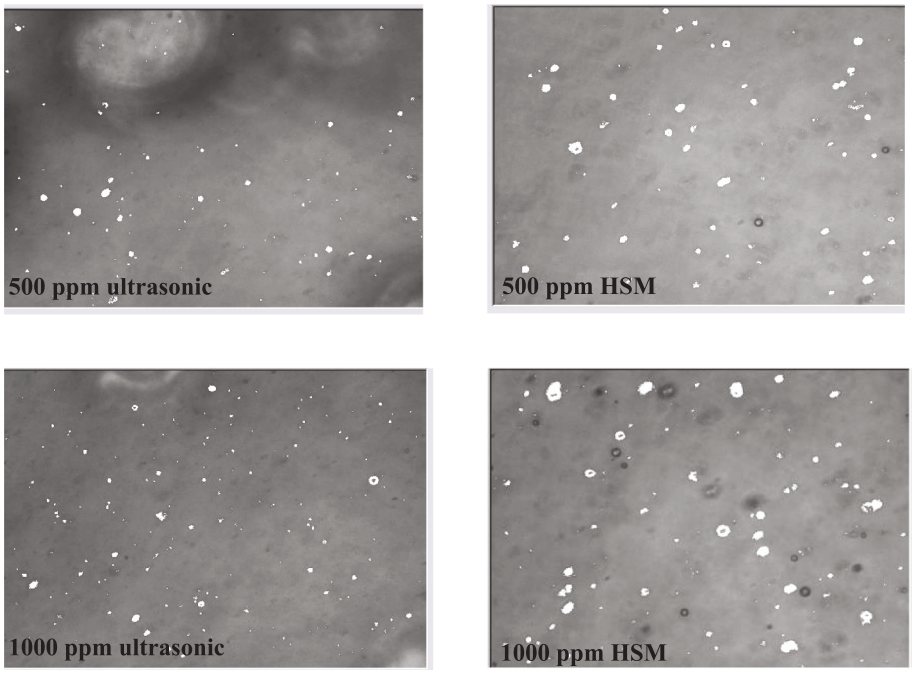

Fig. 3. Image captured of dispersed water droplets on initial mixing Jet A-1 fuel with the high shear mixer and ultrasonic horn.

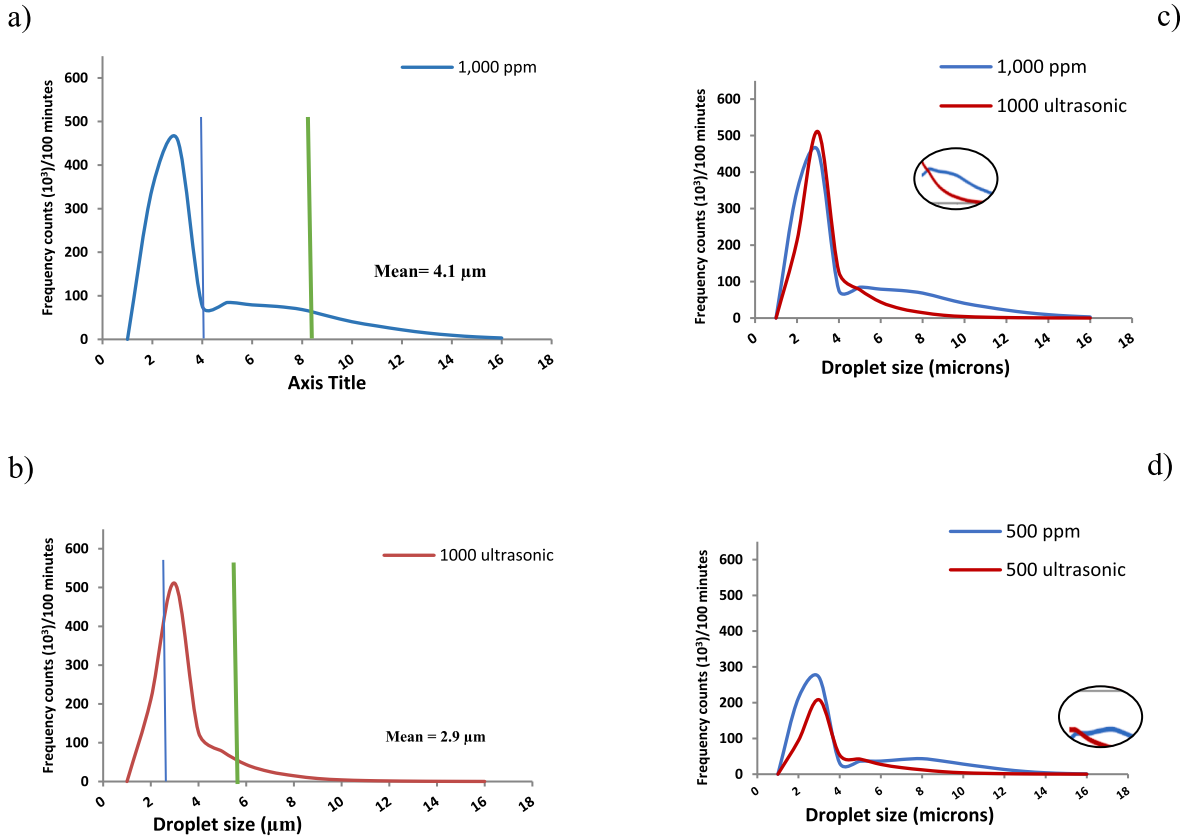

Fig. 4. a and b; DSD (with smoothened kernels for phase 1 experiments). The blue vertical bar is the average diameter of the droplets. The green vertical bar is the average WVA; c and d; comparison and evidence of repeatability for all shearing experiments. (For interpretation of the references to colour in this figure legend, the reader is referred to the web version of this article.)

produced in the ultrasonically dispersed fuel/water mixture.

Additionally, the results shearing experiments shows that there is a decrease in the droplets count over time. However, the rate of decrease is faster after a mild shearing effect, compared to the higher shearing effect ultrasonic horn. In contrast, a slight increase in the average droplets size with timeis noticeable for the HSM mixture in Fig. 5c whilst

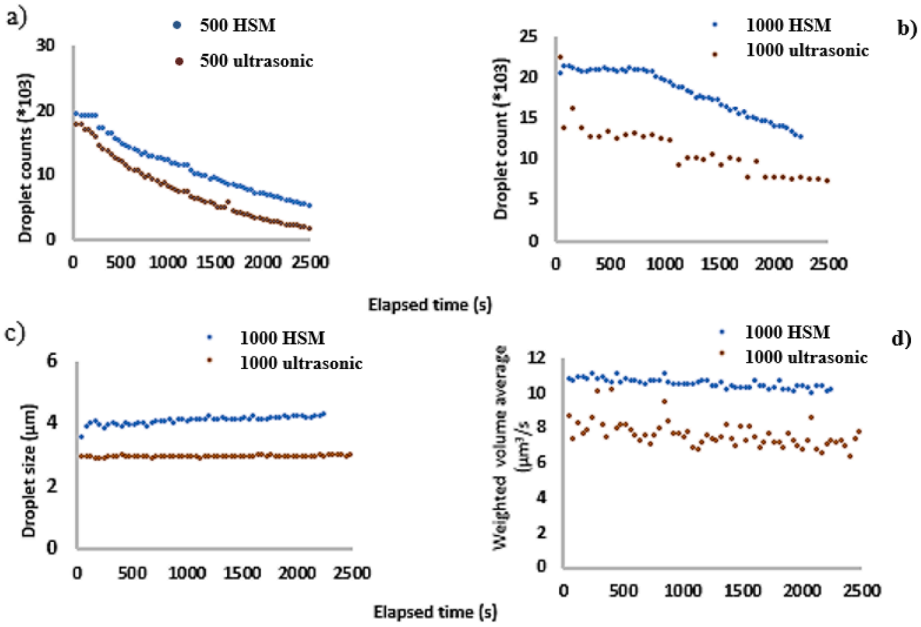

Fig. 5. Water droplets count a) settling profile for jet fuel/500 ppm dispersed water mixture produced ultrasonically and that produced with the high shear mixer; b) settling profile for jet fuel/1,000 ppm dispersed water mixture produced ultrasonically and that produced with the high shear mixer; c) shearing effect on droplets size; a high-intensity shearing effect such as the use of the ultrasonic horn produces tighter emulsions hence the smaller droplets diameter; d) shearing effect on the weighted volume average (volume of droplets).

there is no significant change in the droplets diameter overtime with the UPs mixture. This increase in droplets size over time, could be attributed to the coalescence phenomenon.

The cumulative frequency (CF) distribution represented in Fig. 6 shows some similarity in the median diameter (d50, CF of 50 %) of both shearing methods in the 500 ppm case. However, very minimal change in the 1000 ppm case was seen. 3–4 µm sized droplets are seen to have a CF of 80 % for the ultrasonic case. However, at the same CF of 80 %, 6–7 µm sized droplets are seen for the HSM case. The DSD shows that there exists a higher frequency of larger droplets in the HSM case in comparison to that of the ultrasonic. This could mean that the ultrasonic case produces a more stable emulsion with better homogenising effect. A notable point from Figs. 4, 5 and Table 2 is that the highest value of volume-weighted mean and mean diameter is reached on shearing with the high shear mixer.

From Table 2, hexanol, which is likely to form a very stable mixture has the highest kurtosis and skew value of 34.90 and 5.07, respectively. This further means that a more stable mixture was formed using the ultrasonic processor. From a practical point of view, the right choice of emulsification is essential in obtaining a stable mixture. Therefore, from this work, it can be concluded that mild shearing conditions could be beneficial as it promotes droplets coalescence, leading to a faster/ better separation ability. Whilst the high intensity shearing conditions leads to a tighter emulsion hence resulting in poor water separation.

Table 2
Result data summary for shearing experiments explored for this work, compared with a hexanol/water mixture.

Shear condition	Kurtosis parameter	Skew parameter	Average diameter $D_{1,0}$ (µm)	WVA $D_{4,3}$ (µm)	Average droplets count
Ultrasonic processor	13.45	3.57	2.9	7.1	15,000
High shear mixer HSM	7.5	2.86	4.1	10.11	21,000
Hexanol Using HSM	34.90	5.07	2.6	6.3	134

Effects of total water content: It has been established in the literature that ice accretion is dependent on the amount of water in fuel, temperature and size of supercooled water droplets in the fuel [8–10]. Also, Goodarzi et al. suggested that droplets interact with each other and deform from their original spherical shape at increased water

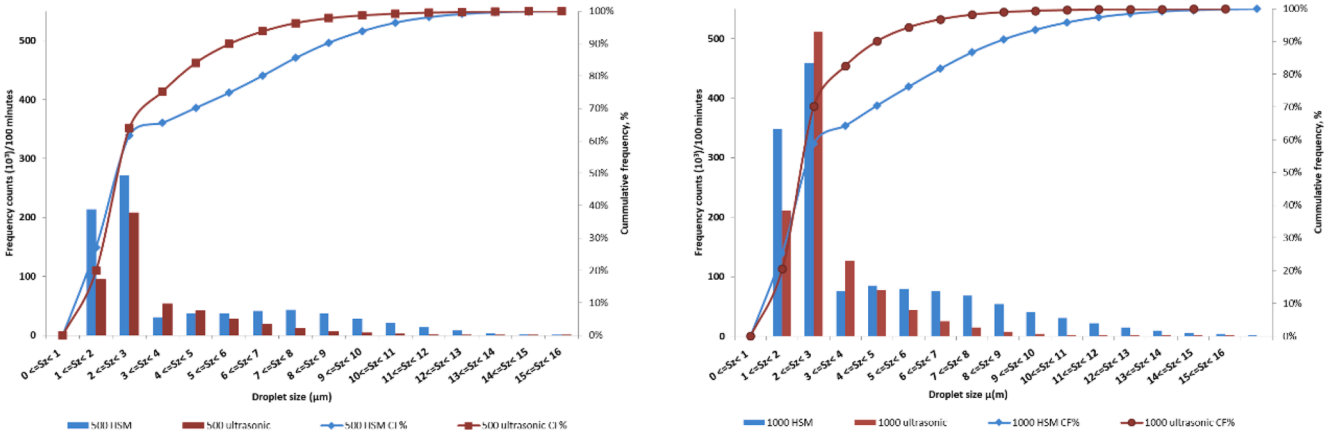

Fig. 6. Cumulative frequency DSD for the different shearing experiments.

concentrations of dispersed phase; the researchers suggested correction factors as a function of the dispersed phase volume fraction to consider the deformation of droplets. The results obtained from work by Goodarzi et al. show that there is a good separation in the water and fuel mixture in fuels with higher total water content [2]. As a result, the influence of water content on the average droplets size distribution is evaluated to demonstrate the impact of water content and time on the water droplets size and count distribution. The choice of added water content was arbitrary for this study; the importance was having a considerable and comparable amounts of free water as free water content can be affected by the total water content of the fuel. The result illustrated in Fig. 7 shows the influence of water content on the droplets size and count. The total droplets count data were plotted against the different total water contents explored in Fig. 7a. The ViPA detected an average count of about 22,079 in the 60 min at 10000 ppm and 1087 at 200 ppm. Count data for the added water test cases show a steady decrease in the order of 10000 > 5000 > 1000 > 500 > 200 > fuel as received.

Fig. 7b shows the water settling rate profile for the added water content in aviation fuel. The settling profile illustrates that total added water content could impact water-shedding rates. As seen in Fig. 7b, there is more driving force for the water to come out of suspension at higher nominal water levels, particularly shortly after mixing. This result is consistent with the proportionality seen in Fig. 8a. This is because the rate at which water droplets will fall out of a solution is dependent on the droplets volume concentrations and the square of the diameter. As seen from Fig. 8a, water droplets fall out at a higher rate in the 10000 ppm case because of the larger droplets compared to other lower total added water cases. These shows that the water droplets data is consistent with theoretical assumptions that droplets size impacts water-shedding rates.

Results observed in Fig. 8 are consistent with the proportionality shown in Fig. 7 as the 10000 ppm case has the highest droplets count, WVA and droplets size diameter. Therefore, it is noticeable from Figs. 7 and 8 that larger water droplets and count are formed with a higher total water content level. The detected water droplets sizes for all phase 2 experiments are given in Appendix 1.

Fig. 9 shows screenshots from the ViPA, illustrating that droplets size and count reduces over time. The lower droplets counts over time is because of droplets settling, with a steady decrease of count and water concentration expected as time progresses (see Fig. 10 is in the text).

Evidently, as volume concentrations are principally based on the mass equivalent, the 10000ppm case contains the highest frequency of both smaller and larger droplets in comparison to all other added water cases. The results from this section explain why keeping the water present in jet fuel at a minimal level is highly important to prevent large volume/size of droplets forming in fuel tanks and potentially causing problems at high altitudes.

4. Water droplets- free and hindered settling velocity

The first step towards having an idea of the size of droplets formed is to consider the emulsion as undergoing a free settling process, (i.e., only one water droplet is settling through the continuous phase of fuel). A process is termed free settling when a particle is at a sufficient distance from the walls of the container and from other particles so that its fall is not affected by the walls or other particles. Stokes law equation gives an idea of the size of droplets that can exisit in a particular emulsion. For a spherical particle settling freely, a droplet of mass 'm' is assumed to fall under gravity at a constant velocity (terminal velocity). Stokes law is used to calculate the terminal velocity for a given droplet size. The resulting terminal velocity is proportional to the square of the droplet diameter. Stokes Law is given as follows:

$$v = \frac{g \cdot D^2(\rho_w - \rho_f)}{18 \cdot \eta_f \cdot \rho_f} \tag{5}$$

where

ρ_p = density of water (kg/m^3).
s = density of fuel (kg/m^3).
g = acceleration due to gravity (m/s^2).
η_f = kinematic viscosity of fuel (m^2/s).
V = Stokes terminal velocity (m/s).
D = Water droplet diameter (m).

For a free settling calculation, it was assumed that terminal velocity was reached i.e., acceleration time is neglected, flow is laminar with a low settling velocity, Reynolds number of Re < 0.2 and that droplets particles are spherical, smooth, and rigid.

For this work, the measured water WVA was used to calculate the terminal velocity, then a graph that describes the relationship between terminal velocity and the WVA for the different water concentrations conducted is shown in Fig. 9.

This relationship was obtained using Stokes law. Fig. 11 above shows how the droplets diameter varies with water concentration, and the effect on terminal velocity. It is evident that the terminal velocity increases with increasing concentration as a result of the increase in WVA. This is consistent with work from literature that suggested that settling

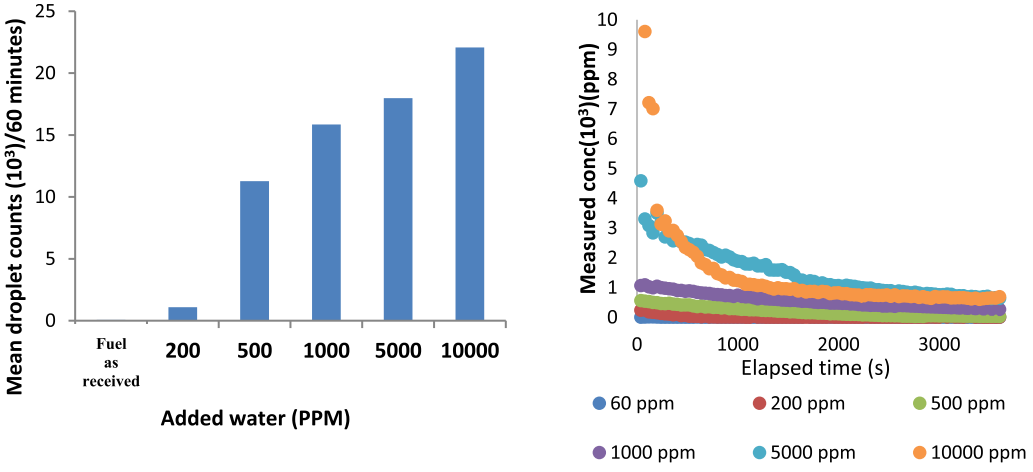

a) b)

Fig. 7. a Estimated average droplet count of added water. b Measured water settling rate content.

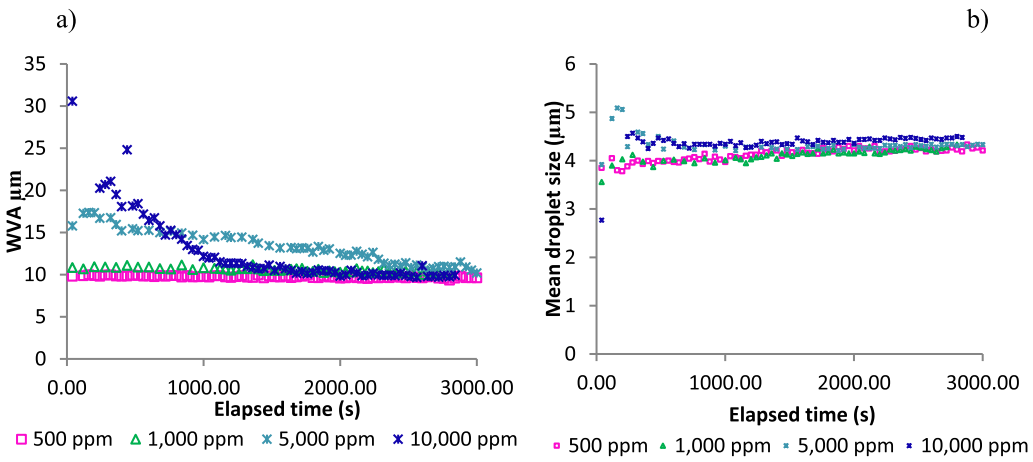

Fig. 8. Shows the a) weighted volume average data against time; b) Mean droplets size against time for test cases c.1 to case c.6.

velocities are affected by high concentrations (Baldock et al). However, Stokes law accounts for a single perfectly spherical droplet falling freely in a medium, neglecting the effect of water concentration in hindered settling (which is the likely typical scenario). In hindered settling, the particles or droplets will have a much lower settling rate or velocity than particles in free settling because of interactions crowded droplets. One widely accepted factor that accommodates the concentration term is given by Richardson and Zaki [29]. This semi-empirical equation for hindered settling is given below:

$$U = V(1 - C)^{n} \quad (6)$$

where

U: Settling velocity, m/s.

V: Stokes terminal velocity, m/s.

n: Ranges from 2.4 to 4.65 for increasing particle Reynolds Number.

C: Volume concentration.

It is therefore proposed that models that could be used to account for the effect of water concentration and settling be developed. Some proposed suggestions have been listed in Table 3 below. It is recommended that more experiments be done to modify the empirical correlations to fit the test with water droplets since the index exponents for some of the experiments are for solid particles.

5. Conclusions and recommendations

Experimental data reveals that water droplets size/count distribution is influenced by the type of shearing/mechanical agitation used during water introduction method. Mild shearing conditions (HSM in this case) could help promote droplets coalescence, leading to better separation ability. The droplets size distribution for mixtures with higher shear conditions (ultrasonic horn) is characterised by their near monomodal (single peak) distribution and a slightly higher kurtosis value of 13.45. Droplets size distribution for a mixture created with mild shear is characterised by an almost-evident second peak and a lower kurtosis value. Also, the skewness value is lower for the high shear mixer distribution compared to the ultrasonic horn distribution. Therefore, on mixing with the ultrasonic horn, a high intensity shearing effect is generated as it introduces a lot of energy into the system.

Furthermore, very minimal change in the 1000 ppm added water concentration was seen.3–4 µm sized droplets has a CF of 80 % for the ultrasonic case. However, at the same CF of 80 %, 6–7 µm sized droplets are seen for the HSM case. Observations from the DSD shows that there exists a higher frequency of larger droplets in the HSM case in comparison to that of the ultrasonic. This could mean that the ultrasonic case produces a more stable mixture with better homogenising effect.

Droplets coalescence phenomenon was evident in the shearing phase 1 experiments with the high shear mixer (medium energy input in this case). Mild shearing conditions promote droplets coalescence, leading to a better separation ability. From a higher energy input to medium energy input, DSD changed significantly in terms of mean values and the higher skewness and kurtosis value.

The present study recommends the parametric studies of the exponent for hindered settling velocity. Hindered settling velocity for water droplets could be formulated using the Richardson and Zaki equation. Therefore, further research should be carried out to develop a new empirical model to account for water droplets in a hindered settling scenario. Also, it is suggested that an independent experimental data set be collected to validate the model formulated in this study. It is further recommended that the experiments be replicated to simulate temperature of an aircraft in service.

6. Funding sources

This work was funded by EPSRC-UKRI (Reference ID: EP/N509127/1) and Airbus Operations, Filton, Bristol (Reference ID: 1100152106), United Kingdom.

7. Availability statement

The data that support the findings of this study are available in the Cranfield Online Research Data (CORD) repository at https://10.17862/cranfield.rd.19067666.

CRediT authorship contribution statement

Judith Ugbeh-Johnson: Writing – review & editing, Data curation, Resources, Conceptualization, Visualization, Formal analysis. **Mark Carpenter:** Supervision, Formal analysis, Validation, Funding acquisition, Methodology, Visualization, Writing – review & editing. **Nonso Evaristus Okeke:** Conceptualization, Formal analysis, Visualization. **Nathalie Mai:** Conceptualization, Formal analysis, Visualisation.

Declaration of Competing Interest

The authors declare that they have no known competing financial interests or personal relationships that could have appeared to influence the work reported in this paper.

Data availability

The data that support the findings of this study are available in the Cranfield Online Research Data (CORD) repository at https://doi.org/

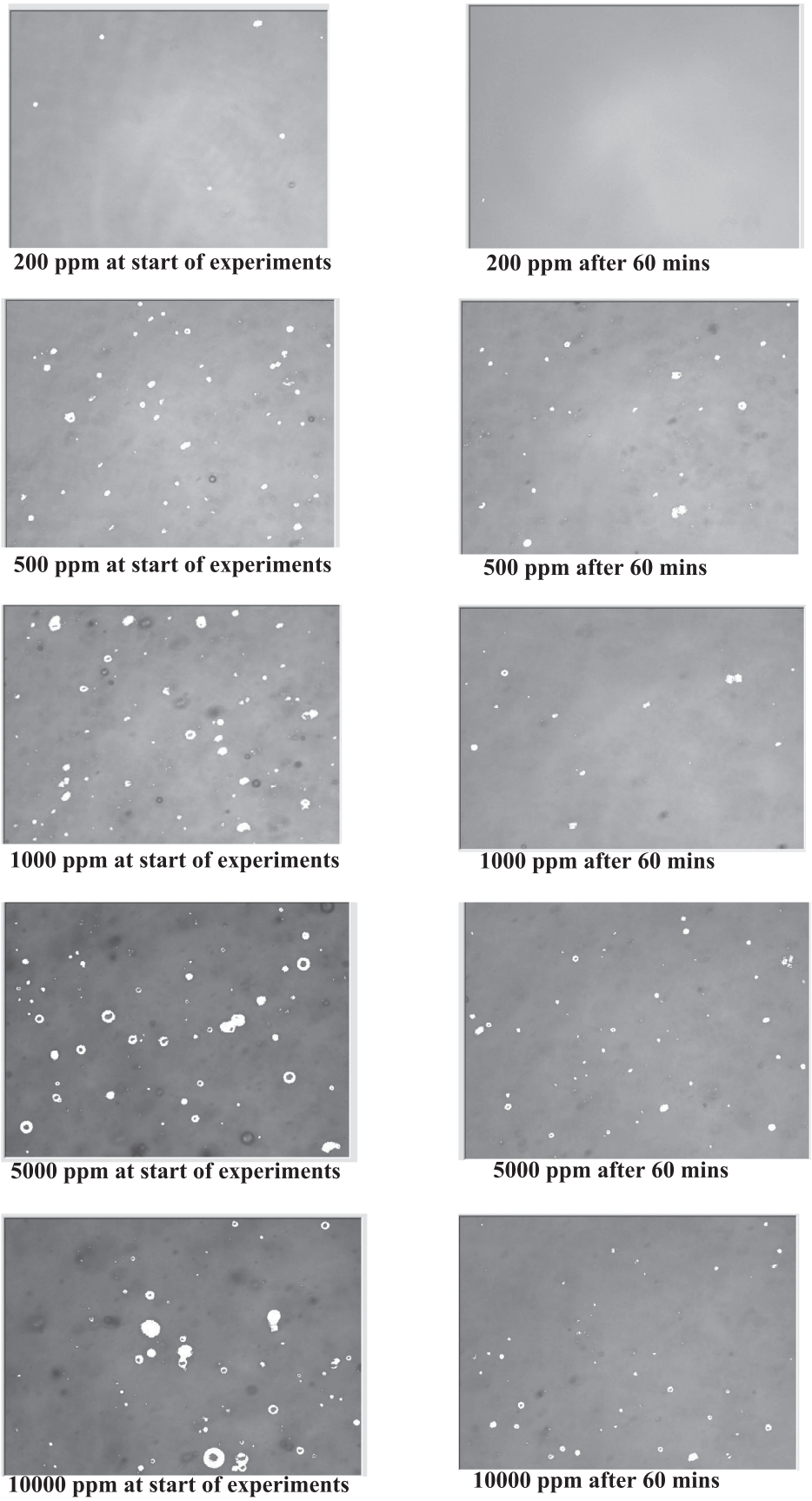

Fig. 9. Captured ViPA images at the start (after ~2 min) and end (after ~60 min) of experiment.

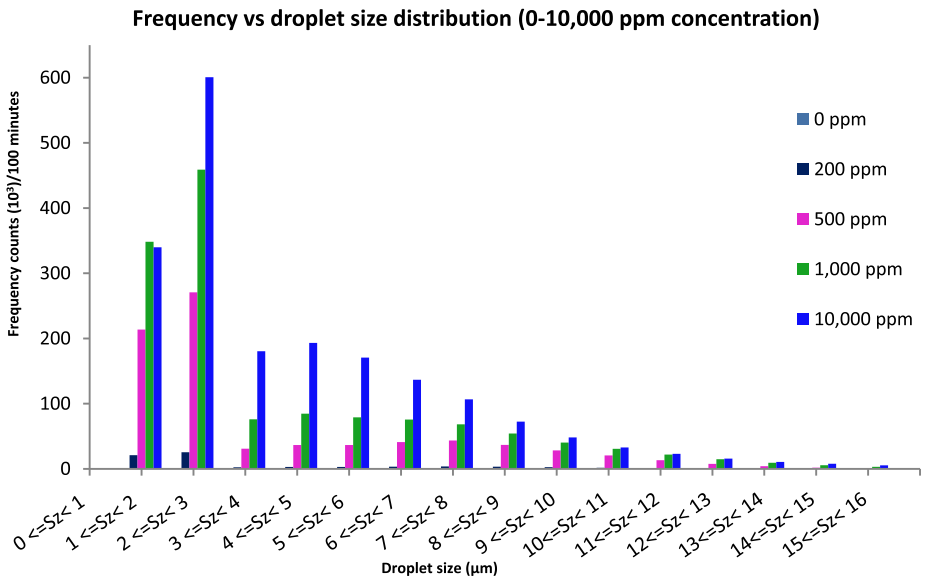

Fig. 10. Comparative analysis of the frequency distribution for the total water content explored for this work (Case c.1 to c.5).

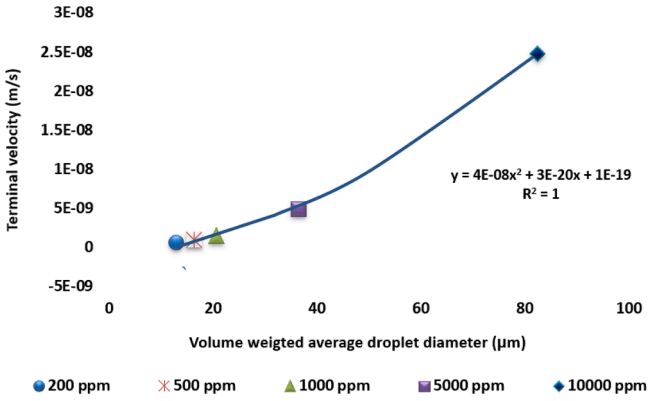

Fig. 11. Relationship between droplet diameter (WVA), water ccincentration and terminal velocity.

Table 3
Semi-empirical correlations that account for water concentration in hindered settling.

S/N	Reference	Formulated model	n value
1	Richardson and Zaki [29]	$U = V(1-C)^n$	n = 4.65
2	Garside and Al-Dibouni [30]	$U = V(1-C)^n$	n = 5.14
3	Al-Naafa and Sami-Selim [31]	$U = V(1-C)^n$	n = 6.55

10.17862/cranfield.rd.19067666

Appendix 1

Appendix 1 shows the detected water droplets sizes for all phase 2 experiments. It is noticeable from the data that larger water droplets and counts are formed with a higher total water content.

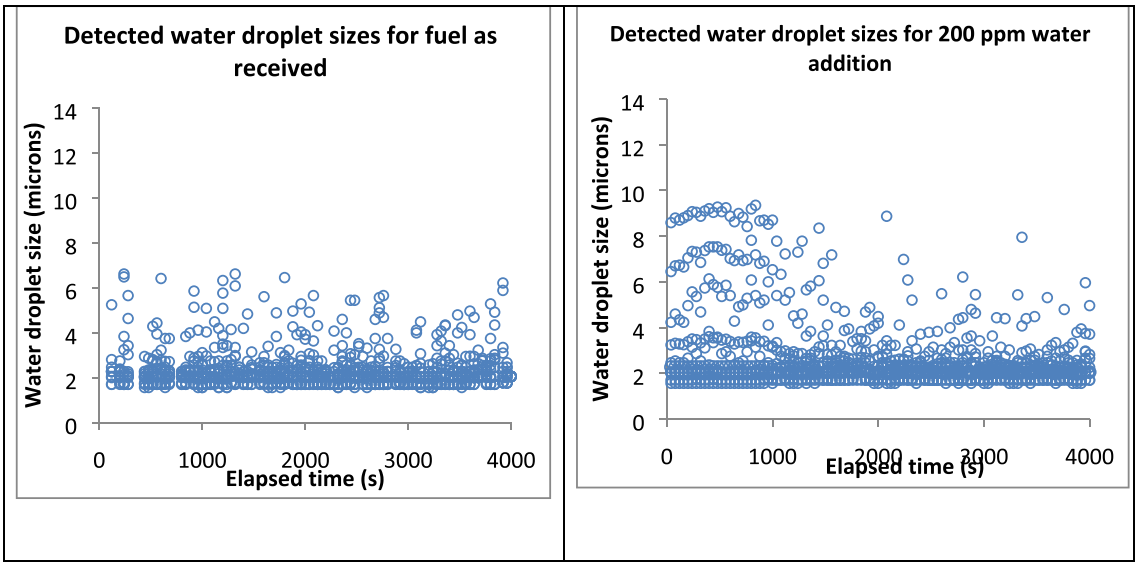
Detected water droplet sizes for fuel as received
Water droplet size (microns)
Elapsed time (s)
Detected water droplet sizes for 200 ppm water addition
Water droplet size (microns)
Elapsed time (s)

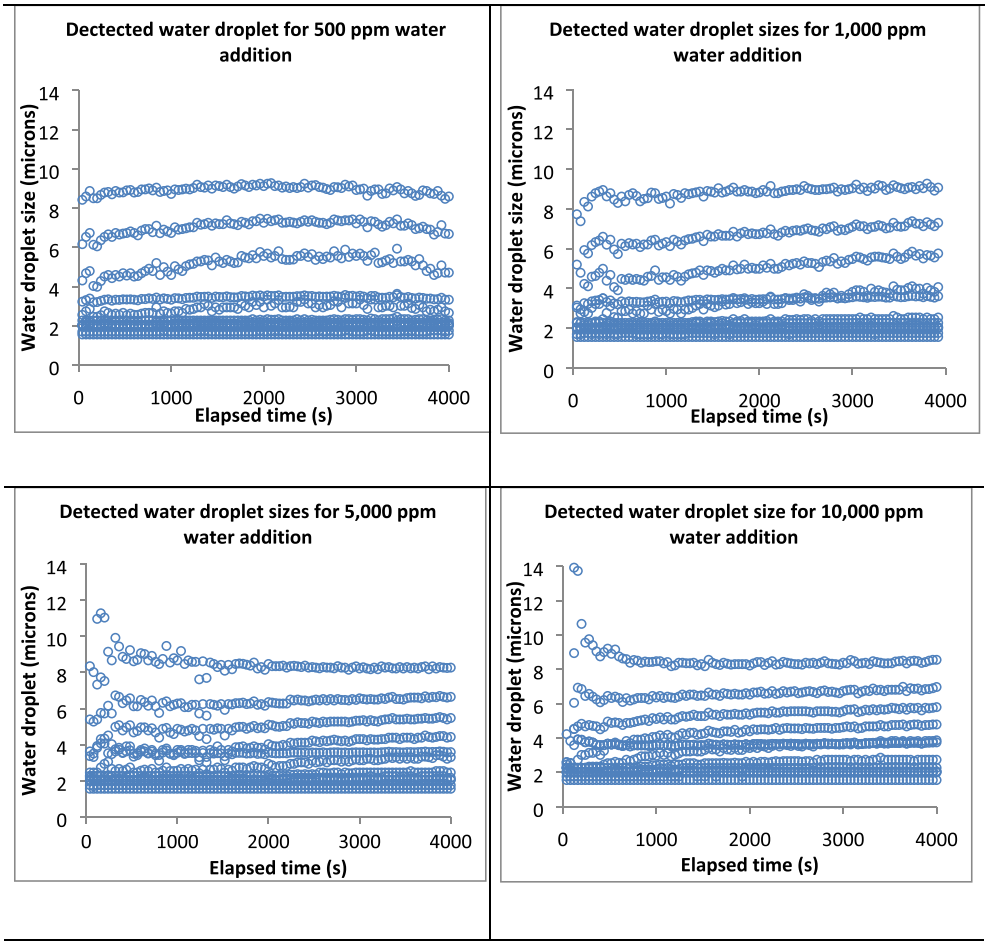
Dectected water droplet for 500 ppm water addition
Water droplet size (microns)
Elapsed time (s)
Detected water droplet sizes for 1,000 ppm water addition
Water droplet size (microns)
Elapsed time (s)
Detected water droplet sizes for 5,000 ppm water addition
Water droplet (microns)
Elapsed time (s)
Detected water droplet size for 10,000 ppm water addition
Water droplet (microns)
Elapsed time (s)

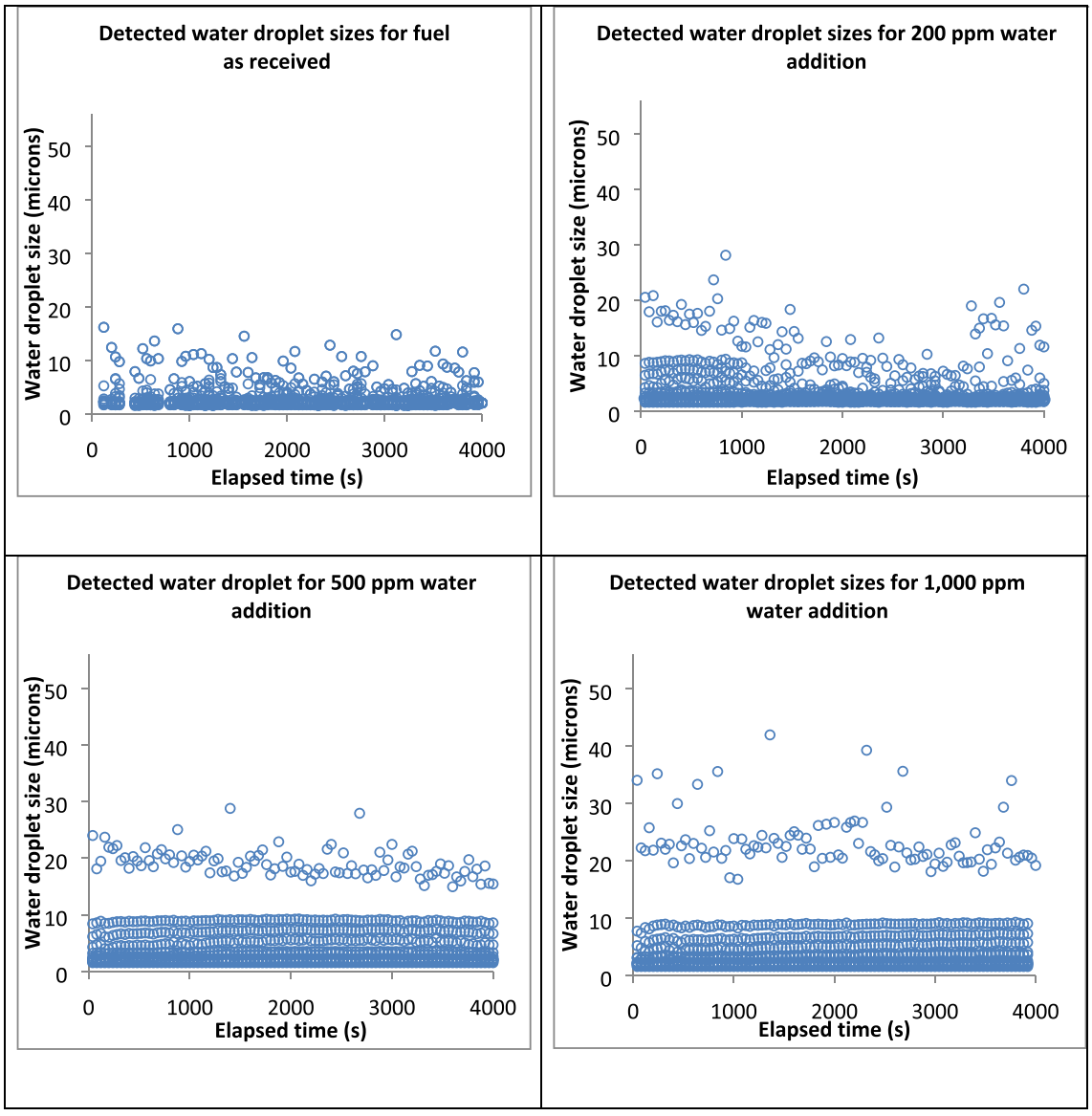
Detected water droplet sizes for fuel as received
Water droplet size (microns)
0
10
20
30
40
50
0
1000
2000
3000
4000
Elapsed time (s)
Detected water droplet sizes for 200 ppm water addition
Water droplet size (microns)
0
10
20
30
40
50
0
1000
2000
3000
4000
Elapsed time (s)
Detected water droplet for 500 ppm water addition
Water droplet size (microns)
0
10
20
30
40
50
0
1000
2000
3000
4000
Elapsed time (s)
Detected water droplet sizes for 1,000 ppm water addition
Water droplet size (microns)
0
10
20
30
40
50
0
1000
2000
3000
4000
Elapsed time (s)

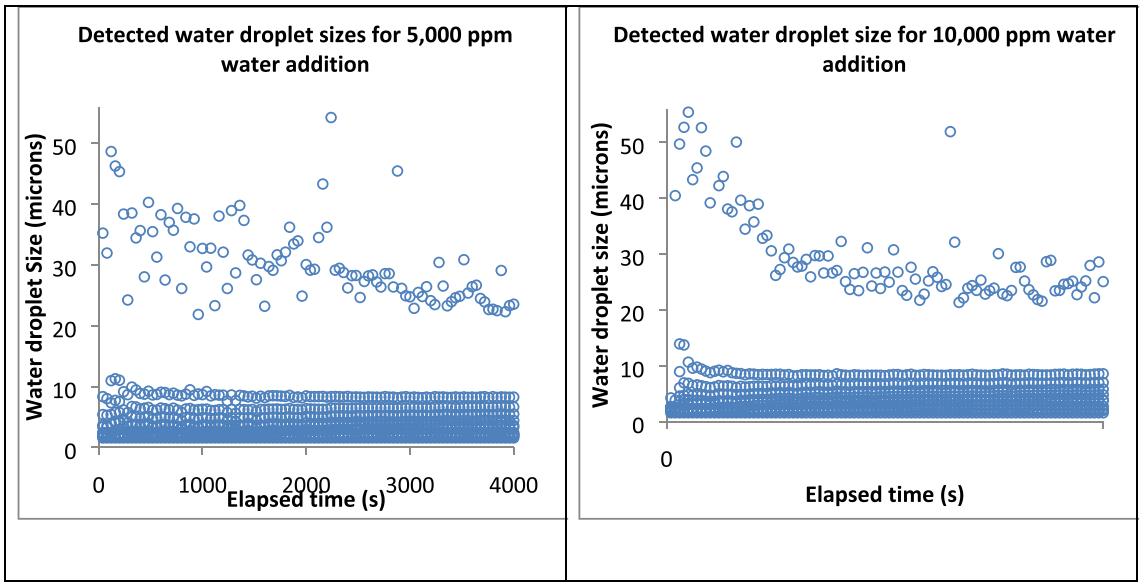

References

[1] Murray BJ, Broadley SL, Wilson TW, Bull SJ, Wills RH, Christensonb HK, et al. Kinetics of the homogeneous freezing of water. Phys Chem Chem Phys 2010: 10380–7. https://doi.org/10.1039/C003297B.

[2] Noor El-Din MR, El-Hamouly SH, Mohamed HM, Mishrif MR, Ragab AM. Water-in-diesel fuel nanoemulsions: preparation, stability and physical properties. Egypt J Pet 2013;22:517–30. https://doi.org/10.1016/j.ejpe.2013.11.006.

[3] Goodarzi F, Zendehboudi S. A comprehensive review on emulsions and emulsion stability in chemical and energy industries. Can J Chem Eng 2019;97:281–309. https://doi.org/10.1002/cjce.23336.

[4] Morgan VG, Sad CMS, Constantino AF, Azeredo RBV, Lacerda V, Castro EVR, et al. Droplets size distribution in water-crude oil emulsions by low-field NMR. J Braz Chem Soc 2019;30:1587–97. https://doi.org/10.21577/0103-5053.20190057.

[5] Stewart M, Arnold K, Produced Water Treating Systems, in: Prod. Water Treat. F. Man., Elsevier, 2011: pp. 1–134. 10.1016/B978-1-85617-984-3.00001-8.

[6] Pires APP, Han Y, Kramlich J, Garcia-Perez M. Alternative jet fuel properties. BioResources 2018;13:2632–57.

[7] ElGalad MI, El-Khatib KM, Abdelkader E, El-Araby R, ElDiwanib G, Hawash SI. Empirical equations and economical study for blending biofuel with petroleum jet fuel. J Adv Res 2018;9:43–50. https://doi.org/10.1016/j.jare.2017.10.005.

[8] Baena S, Repetto SL, Lawson CP, Lam W, Behaviour of water in jet fuel a literature review, 60 (2013) 35–44.

[9] Chan KY, Lam J-W. Water drop runoff in aircraft fuel tank vent systems. Proc Inst Mech Eng Part C J Mech Eng Sci 2017;231(24):4548–63.

[10] Naya S, Cao R, Francisco-Fernández M, Tarrío-Saavedra J, Brage H, Cancelo C. Estimating water and solid impurities in jet fuel from ISO codes. Energy Fuels 2013. https://doi.org/10.1021/ef401378z.

[11] Charro A, Baena S, Lam JK. Water solubility in different alternative jet fuels: a comparison with petroleum-based jet. Fuel 2015. https://doi.org/10.4271/2015-01-2563.

[12] Elliott JW, Smith FT. Ice formation on a smooth or rough cold surface due to the impact of a supercooled water droplets. J Eng Math 2017;102:35–64. https://doi.org/10.1007/s10665-015-9784-z.

[13] Miller AJ, Brennan KP, Mignani C, Wieder J, David RO, Borduas-Dedekind N. Development of the drop Freezing Ice Nuclei Counter (FINC), intercomparison of droplets freezing techniques, and use of soluble lignin as an atmospheric ice nucleation standard. Atmos Meas Tech 2021;14. https://doi.org/10.5194/amt-14-3131-2021.

[14] Bernstein BC, Wolff CA, McDonough F. An inferred climatology of icing conditions aloft, including supercooled large drops. Part I: Canada and the continental United States. J Appl Meteorol Climatol 2007;46:1857–78. https://doi.org/10.1175/2007JAMC1607.1.

[15] Bernstein BC, Le Bot C. An inferred climatology of icing conditions aloft, including supercooled large drops. Part II: Europe, Asia, and the Globe. J Appl Meteorol Climatol 2009;48:1503–26. https://doi.org/10.1175/2009JAMC2073.1.

[16] Xu Y, Petrik NG, Smith RS, Kay BD, Kimmel GA. Homogeneous nucleation of ice in transiently-heated, supercooled liquid water films. J Phys Chem Lett 2017;8: 5736–43. https://doi.org/10.1021/acs.jpclett.7b02685.

[17] Ugbeh Johnson J, Carpenter M, Williams C, Pons J-F, McLaren D. Complexities associated with nucleation of water and ice from jet fuel in aircraft fuel systems: a critical review. Fuel 2022;310:122329. https://doi.org/10.1016/j.fuel.2021.122329.

[18] Zhang W, Webb DJ, Carpenter M, Williams C. Measuring water activity of aviation fuel using a polymer optical fiber Bragg grating. in 2014. https://doi.org/10.1117/12.2059273.

[19] Zhang C, Chen X, Webb DJ, Peng G-D, Water detection in jet fuel using a polymer optical fibre Bragg grating, in: 20th Int. Conf. Opt. Fibre Sensors, 2009: p. 750380. 10.1117/12.848696.

[20] Maloney TC, Diez FJ, Rossmann T. Ice accretion measurements of Jet A-1 in aircraft fuel lines. Fuel 2019;254:115616. https://doi.org/10.1016/j.fuel.2019.115616.

[21] Schmitz M, Schmitz G. Experimental study on the accretion and release of ice in aviation jet fuel. Aerosp Sci Technol 2018;82–83:294–303. https://doi.org/10.1016/j.ast.2018.08.034.

[22] McClain ST, Zhang T, Ahmed SU, Stafford G, Cornejo JA, O'neal DL, A climatic facility and apparatus for investigations of cold soaked fuel frost evolution, in: AIAA Aviat. 2020 FORUM, 2020. 10.2514/6.2020-2808.

[23] Clark AQ, Smith AG, Threadgold S, Taylor SE. Dispersed Water and Particulates in Jet Fuel: Size Analysis under Operational Conditions and Application to Coalescer Disarming. Ind Eng Chem Res 2011;50:5749–65. https://doi.org/10.1021/ie102533e.

[24] Bessee G, Determination of water droplets size distributions in diesel and aviation fuels, in: 13th Int. Conf. Stability, Handl. Use Liq. Fuels 2013, 2013: pp. 267–272.

[25] Ugbeh-Johnson J, Carpenter M, Okeke N-E, Nnabuife SG, Mai N. Investigation of water droplets size distribution in conventional and sustainable aviation turbine fuels. SAE Int 2022. https://doi.org/10.4271/04-15-03-0016.

[26] Wedd M, Particle size analysis, in: Encycl. Anal. Sci. Second Ed., Elsevier, 2004: pp. 18–29. 10.1016/B0-12-369397-7/00439-8.

[27] I. Standard, ISO 9276-2: Representation of results of particle size analysis— Part 2: Calculation of average particle sizes/diameters and moments from particle size distributions, Int. Stand. ISO 9276-2. 2002 (2002).

[28] Westfall PH, Kurtosis as peakedness, 1905–2014. R.I.P., Am. Stat. 68 (2014) 191–195. 10.1080/00031305.2014.917055.

[29] Richardson JF, Zaki WN. The sedimentation of a suspension of uniform spheres under conditions of viscous flow. Chemical engineering science 1954. https://doi.org/10.1016/0009-2509(54)85015-9.

[30] Garside MR, Al-Dibouni J. Velocity-voidage relationships for fluidization and sedimentation in solid-liquidsystems. Ind Eng Chem Res 1977;16:206–14.

[31] Al-Naafa M, Sami Selim MA. Sedimentation of monodisperse and bidisperse hard-sphere colloidalsuspensions. AIChe 1992;38:1618–30.

Characterization of water droplets size distribution in aviation turbine fuel: ultrasonic homogeniser vs high shear speed mixer

Ugbeh-Johnson, Judith

2023-01-15

Ugbeh-Johnson J, Carpenter M, Okeke NE, Mai N. (2023) Characterization of water droplets size distribution in aviation turbine fuel: ultrasonic homogeniser vs high shear speed mixer, Fuel, Volume 332, Part 1, January 2023, Article number 125674

https://doi.org/10.1016/j.fuel.2022.125674